Scaling of saturated stimulated Raman scattering with temperature and intensity in ignition scale plasmas

R. K. Kirkwood, R. L. Berger, C. G. R. Geddes, J. D. Moody, B. J. MacGowan, S. H. Glenzer, K. G. Estabrook, C. Decker, and O. L. Landen
University of California, Lawrence Livermore National Laboratory, Livermore, California 94551

(Received 18 December 2002; accepted 9 April 2003)

Measurements show the scaling of stimulated Raman scattering (SRS) with laser intensity and plasma electron temperature under the conditions expected in ignition experiments. The scaling of the scattered energy with each parameter follows a power law with a small exponent (of order 1). Comparison with simulations suggests SRS is nonlinearly saturated in these cases. Further experiments with high Z dopants showed that the effect of electron-ion collisions on the measured SRS is primarily due to the inverse bremsstrahlung absorption of the scattered light. © *2003 American Institute of Physics.* [DOI: 10.1063/1.1580814]

I. INTRODUCTION

Reliable prediction of the stimulated Raman (SRS) and Brillouin scattering (SBS) in plasmas expected in indirectly driven inertial confinement ignition schemes[1] is critical to its success. The plasma and laser parameters make it difficult to remain below the linear thresholds of filamentation and the three wave resonant backscatter instabilities, SRS and SBS in present target designs.[1] In fact, the SRS and SBS linear gain exponents (>20)[2,3] are large enough that nearly total reflection of the incident light would be predicted without accounting for the nonlinear response of the plasma. In previously reported experiments conducted on the Nova laser facility with plasma and laser conditions similar to the present study, SRS was found to increase with the fraction of low-Z ions in the plasma,[4,5] most likely indicating a dependence on the damping rate of the acoustic wave in multispecies plasma.[6] Because linear SRS growth rates do not depend on this acoustic wave damping rate but the Langmuir decay instability (LDI) threshold does increase with the acoustic wave damping rate,[7–9] this dependence has been interpreted as evidence that LDI limited the amplitude of the SRS-driven Langmuir wave and thus SRS as well. More direct evidence of LDI has come from Thomson scatter from the LDI decay products, both from the acoustic wave[10] and the Langmuir wave[11] in exploding foil plasma and from the acoustic wave in high temperature plasmas.[12,13] Further experiments with intersecting beams have shown the Langmuir waves involved in SRS to be nonlinearly saturated.[14]

One difficulty with this interpretation is the rather high threshold for LDI in Nova plasmas where the electron Landau damping of Langmuir waves and ion Landau damping of the acoustic waves is so strong that the calculated Langmuir wave amplitude remains below the LDI threshold even when SRS is large. It has been suggested that the electron Landau damping may be much lower than assumed because an inverse bremsstrahlung-heated velocity distribution can have a super-Gaussian form[15] which has many fewer electrons near the phase velocity of the Langmuir wave than a Maxwell–Boltzmann distribution with the same kinetic energy.[4,16] Recent measurements of Thomson scattering from thermal electron plasma fluctuations[17] in a high Z plasma find spectra that are best modeled with a spatially uniform super-Gaussian shape for the subthermal electrons and a Maxwell–Boltzmann for the suprathermal electrons. Furthermore, Fokker–Plank calculations[18] that include electron-electron collisions show for Nova-like plasmas that the high velocity electrons responsible for damping Langmuir waves have a Maxwellian tail even if the low velocity electrons are non-Maxwellian. The two component distribution that fits the data might also represent an average over a strongly non-Maxwellian distribution in localized hot spots of the laser, and a less distorted distribution in parts of the scattering volume in which the intensity is lower. These considerations make it apparent that, even with the presence of a substantial population of nonthermal electrons, the damping may not be reduced as much as we will show is needed to model SRS saturation with LDI only.

Another nonlinear plasma response to SRS-produced Langmuir waves is trapping of electrons near the phase velocity which can alter the damping rate[19] and the frequency.[20] Recent particle-in-cell simulations predict that SRS will saturate by LDI for low temperature or high density ($k\lambda_{de}<0.15$) and by particle trapping for high temperature or low density ($k\lambda_{de}>0.25$).[21] Here k is the wavenumber of the Langmuir wave and λ_{de} is the electron Debye length. In linear theory, the ratio ν_e/ω_e of the Landau damping rate, ν_e, to the frequency, ω_e, of a Langmuir wave is a function of $k\lambda_{de}$ only. In nonlinear theory, the frequency and damping also depend on the "bounce" frequency, $\omega_b = kv_{tr} \sim (\delta n_{lw})^{1/2}$ where δn_{lw} is the amplitude of the Langmuir wave. In Vu *et al.*[21] the SRS saturation is attributed to a detuning or frequency shift of the Langmuir wave from the frequency of the beat ponderomotive force of the light waves. Other simulations[22] with a Vlasov code have observed a sideband instability which grows at rate proportional to the bounce frequency and drains power from the primary Langmuir wave that Raman scatters the light, thus saturating SRS.

 © 2003 American Institute of Physics

Downloaded 21 Nov 2003 to 128.32.113.135. Redistribution subject to AIP license or copyright, see http://ojps.aip.org/pop/popcr.jsp

These particle trapping effects, which do not depend on the acoustic wave damping, do not explain the dependence of SRS on ion acoustic wave damping. Other effects could be responsible. For example, such a dependence can arise from the nonlinear competition between SRS and SBS for laser power.[23] In fluid simulations,[24] the reflectivity of one instability is shown to be reduced by the presence of the other when total reflectivity level is as low as 1%–2%. Anticorrelation of SRS and SBS has been reported in a number of experiments, including Nova experiments on gasbags[25] similar to the ones reported here. In those Nova experiments, the SRS was seen to increase with the gas-fill density whereas the SBS decreased. Other experiments on hohlraums with large SRS and very little SBS have reported on a weak SRS scaling with electron density.[26]

With such a complex system with several (not completely satisfying) interpretations published, it is of great value to vary the external parameters believed to play the principal roles in determining the nonlinear state of SRS to test and inspire theoretical insight. In the past, the scaling with electron density and plasma composition has been reported. Here, we report the scaling with laser intensity and electron temperature. We emphasize that the scaling of SRS as a convective three wave instability with an exponential dependence of the reflectivity on the gain exponent is not being tested in this experiment. Even at the lowest intensities used in these experiments, the linear gain exponent for SRS is sufficient to account for greater reflectivity than observed. When the role of laser hotspots is included, it has been shown that there is a critical (spot-averaged) intensity below which there is insignificant backscatter and above which the plasma response is nonlinear.[27,28] Experiments that measured the intensity dependence of SBS in weakly damped gasbag plasmas[29] and SRS in toroidal hohlraums[26] have observed this sudden onset. In Sec. II we will describe experiments studying the dependence of SRS on the beam intensity, and with the aid of simulations will interpret it in the context of the many processes described earlier.

We will also describe experiments in which the dependence on SRS on electron temperature is studied. To aid the understanding of the temperature scaling measurements we also performed measurements when the atomic composition of the plasma was varied. These latter experiments are important because they allow processes that depend on both the ion charge (Z) and the electron temperature (such as electron-ion collisions) to be varied independently from processes that depend only on electron temperature (such as electron Landau damping). In particular, the light absorption rate, $\nu_{\mathrm{abs}}^{0,r}=\omega_{pe}^2\nu_{ei}/2\omega_{0,r}^2$ where the electron-ion collision frequency, $\nu_{ei}=(4\sqrt{2\pi}/3\sqrt{m_eT_e^3})\Sigma_j n_j Z_j^2 e^4 \ln(\Lambda)$, depends on the electron density, n_e, the electron temperature, T_e, and the charge state Z_j and density n_j of each ion species. Hence, the laser light is strongly absorbed in the high-Z plasma but weakly absorbed in the low-Z plasma. Here, m_e is the electron mass, e is the electron charge, n_c is the critical density, and $\ln(\Lambda)$ is the Coulomb logarithm. It is convenient to define

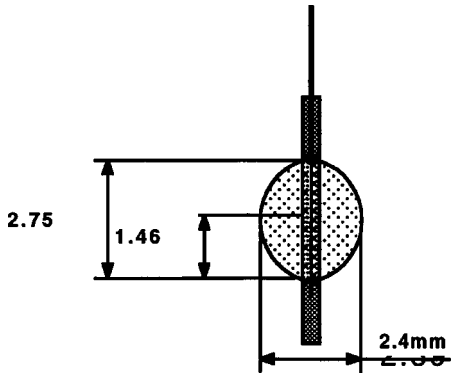

FIG. 1. Schematic of gas filled target used to produce plasmas that are hot and homogeneous by illuminating with nine defocused beams as described in text. The target consists of an approximately spherical CH balloon, mounted in a washer with gas fill tubes.

$$Z=\sum_j n_jZ_j \Big/ \sum_j n_j, \quad \langle Z^2\rangle=\sum_j n_jZ_j^2 \Big/ \sum_j n_j$$

so that the electron-ion collision frequency is proportional to $\langle Z^2\rangle/Z$. In an attempt to separate the effects of the variation of the light wave damping from the plasma wave damping which both vary with T_e, we added Xe to C_5H_{12} plasma to increase the collisional absorption. It is also clear that the SRS light is more strongly absorbed than the incident light because its group velocity is slower and it is closer to its critical density. We will describe the scaling of SRS with Z and compare it with the observed scaling with electron temperature.

II. EXPERIMENTAL DESIGN

The experiments are performed primarily in low-Z CH plasmas produced by pre-heated, gas filled, targets[30,31] at the Nova laser facility. The targets are nearly spherical, thin polyimide bags filled with a gas mixture consisting of two types of CH molecules (C_5H_{12} and C_3H_8) at atmospheric pressure. The target is shown schematically in Fig. 1. The gas is also doped with Ar for x-ray spectroscopic temperature measurements, and also with Xe in the case of collisional damping scaling experiments. A pure C_5H_{12} gas at $\sim$1 atm pressure produces a plasma with an electron density that is 11% of the critical density for the 351 nm laser beams, while a pure C_3H_8 gas at that pressure produces a plasma that is 7.1% of the critical density, and mixtures produce densities in between. The target is pre-heated with nine unsmoothed defocused 351 nm heater beams, each delivering $\leqslant$2.5 kJ in a 1 ns square pulse. The plasma present between 0.5 and 1.0 ns is hot and homogeneous, with an electron temperature of $\sim$3.0 keV at maximum heater energy (determined by spectroscopy measurements[30]) and a nearly 2 mm density plateau inside a radius of 900 μm with rms density perturbations (inferred from Thomson scatter[32]) of less than 5%. The temperature of the plasma is varied by adjusting the heater energy from 1.0 to 2.5 kJ per heater beam. The corresponding plasma temperature is measured by x-ray spectroscopy at each heater energy and confirmed by Thomson scattering from a 263 nm probe beam[31] at the highest heater energy.

Downloaded 21 Nov 2003 to 128.32.113.135. Redistribution subject to AIP license or copyright, see http://ojps.aip.org/pop/popcr.jsp

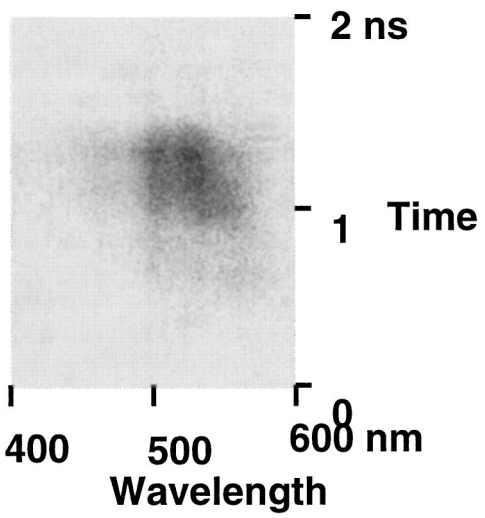

FIG. 2. The time resolved spectrum of the light scattered from a 2×10^{15} W/cm^2 laser beam in a 10% critical density plasma. The wavelength range corresponds to stimulated Raman scattering.

The measured temperature is found to be adjustable from 1.5 to 3.0 keV. A tenth interaction beam with a 1.0 ns square pulse is fired at 0.5 ns. The interaction beam is focused at $r=900\,\mu$m with either an $f/8$ or $f/4.3$ lens, and is conditioned with random phase plates (RPPs) designed with Airy function intensity profiles. Two different RPPs are used in the $f/8$ configuration, one with a best focus FWHM (full width half maximum) of 420 μm, which is used for intensities below $\times10^{15}$ W/cm^2, and a second with a FWHM of 160 μm, which is used for lower intensity experiments, while a third RPP with a FWHM of 120 μm is used in experiments with the $f/4.3$ beam (all spot sizes are calculated for ideal beams with vacuum propagation). The backscattering is measured by a full aperture collection system (FABS) that is sensitive to light inside the laser cone and an imaging system that measures light with scattering angles between the edge of the beam cone (3.6° at f/8 and 6.6° at $f/4.3$), and 18° away from the beam axis, where the fluence is found to be low. The time dependence (resolution ~100 ps) and spectrum of the scattered light in the lens cone is measured by a streaked spectrometer. A time resolved scattered spectrum in the range of $\lambda=400-600$ nm is shown in Fig. 2. In Figs. 3–5, the reflected energy is binned into that collected in the 0.5–1.0 ns "early" period, when the heated plasma is most homogeneous, and the 1.0–1.5 ns "late" period, after the heater beams have turned off and when simulations indicate the plasma is cooling.

III. THE DEPENDENCE OF SCATTERING ON LASER BEAM INTENSITY

The intensity of the interaction beam is varied from 3×10^{14} to 2.5×10^{15} W/cm^2 in experiments with both 7% and 10% critical density targets. The energy collected in the range of the spectrometer at early and late time is used with the incident energy to determine the reflectivity due to SRS, and is plotted in Figs. 3(a) and 3(b). The reflectivity is seen to be almost proportional to laser intensity between 6×10^{14} and 2.5×10^{15} W/cm^2. Further measurements of scattered light in the range of 350–352 nm and attributed to stimulated Brillouin scattering (SBS) are shown in Figs. 3(c) and 3(d). In the "early" period, SBS is small, typically 3%–4% and independent of intensity as is the case for CO_2 gasfills[29] where the acoustic wave damping is weak. LASNEX modeling shows the ion temperature, and thus the ion Landau damping, is lower in this period than in the "late" period when the SBS increases about linearly with laser intensity. The weak scaling of SRS with the interaction beam intensity is consistent with a Langmuir wave response to the ponderomotive force that is less than the predictions based on a linear Langmuir wave response. Evidence that the Langmuir wave response in this case is nonlinear has been observed previously.[14] To investigate further the dependence

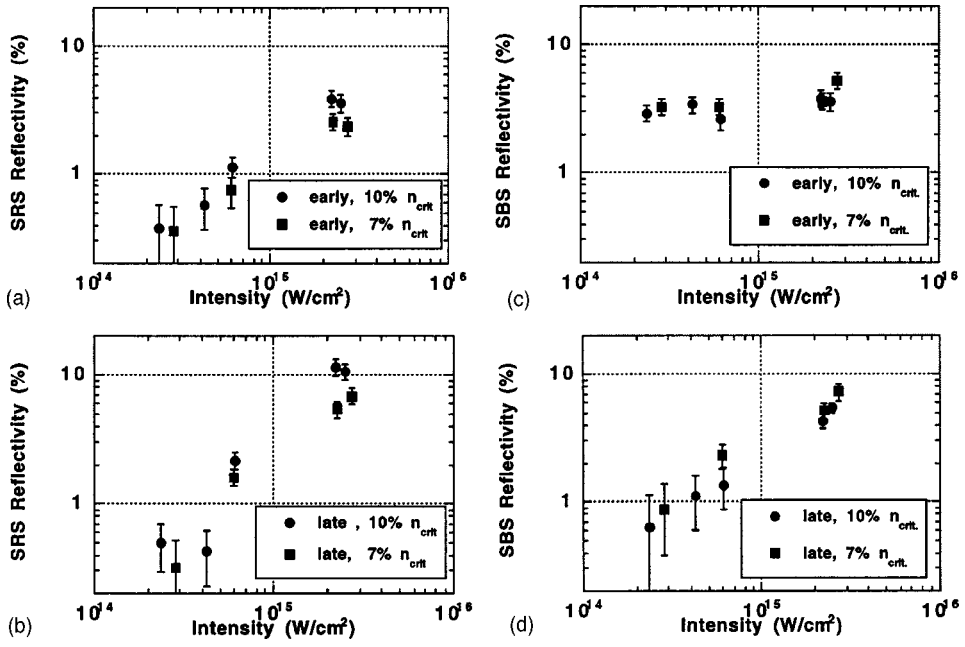

FIG. 3. Laser reflectivity from an $f/8$ beam due to SRS vs the peak vacuum intensity of the random phase plate smoothed $f/8$ beam is shown for the case of 7.1% critical and 10% critical density plasmas and the 0.5–1.0 ns time period (early). (b) Laser reflectivity from an $f/8$ beam due to SRS vs the peak vacuum intensity of the random phase plate smoothed $f/8$ beam is shown for the case of 7.1% critical and 10% critical density plasmas and the 1.0–1.5 ns time period (late). (c) Laser reflectivity from an $f/8$ beam due to SBS for the case of (a). (d) Laser reflectivity from and $f/8$ beam due to SBS for the case of (b).

Downloaded 21 Nov 2003 to 128.32.113.135. Redistribution subject to AIP license or copyright, see http://ojps.aip.org/pop/popcr.jsp

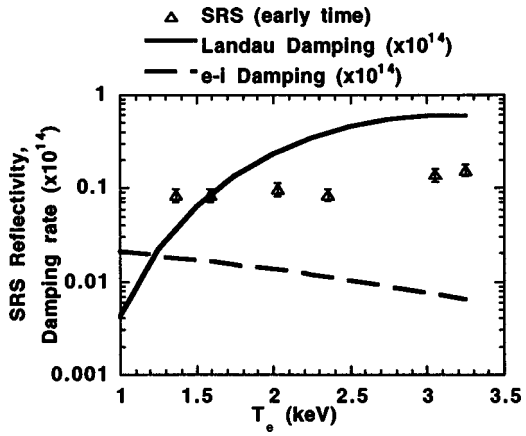

FIG. 4. Laser reflectivity from an $f/4.3$ beam due to SRS vs the electron temperature of an 11% critical density target, measured by x-ray spectroscopy at $r=400\ \mu$m.

on electron temperature we have performed experiments in which the temperature of the plasma is varied.

IV. TEMPERATURE DEPENDENCE OF SRS

The temperature scaling experiments are designed to allow the effects of the variation of the inverse bremsstrahlung absorption rate of the incident (351 nm) and scattered (500–600 nm) light to be accounted for, and the scaling of the scattered light with electron temperature to be identified separately. To do this we use an $f/4.3$ interaction beam that has a region of best focus which is smaller in the axial direction ($\Delta z \sim 516\ \mu$m half width at half maximum) than the inverse bremsstrahlung absorption length, L, of the incident 351 nm light propagating in our plasma conditions ($L_{351} \geqslant 1.4$ mm at $n_e = 10^{21}\,\mathrm{cm}^{-3}$, $T_e \geqslant 1.5$ keV, CH plasma). The beam is then focused to an intensity of $4\times10^{15}\,\mathrm{W/cm}^2$ near the plasma edge ($r=0.9$ mm) in a plasma that is fairly uniform for $r<1.0$ mm and $t<1.0$ ns, so that the incident beam is not substantially absorbed before it reaches the region of best focus and the intensity near best focus is not significantly dependent on the plasma electron temperature. The absorption length of the scattered light is smaller ($L_{527} \simeq 580\ \mu$m at $n_e = 10^{21}\,\mathrm{cm}^{-3}$, $T_e \geqslant 1.5$ keV, CH plasma) due to its longer wavelength. The effect of absorption on the reflectivity is calculated and discussed in the following. The timing and pulse shapes are the same as in the intensity scaling experiment. The target is filled with C_5H_{12} gas with a 1% Ar impurity to produce an 11% critical density plasma in which ion wave damping is strong, which earlier experiments[4,5] indicated would suppress SBS and other secondary decay processes and allow SRS to grow to large values. The temperature of the target plasma is varied by varying the energy in the heater beams. The temperature in the plasma, predicted by simulations, is confirmed by x-ray spectroscopic measurements at a radius of 400 μm in a region adjacent to the interaction region.[30,32] Heater energies in the range of 9.5–22 kJ produce plasmas with electron temperatures in the range of 1.5–3.0 keV. These values of temperature and those used in the figures represent the plasma inside the interaction beam that is heated by both the interaction beam as well as the heater beams. To include the effect of the interaction beam on the temperature, the temperature measured in the region heated only by the heaters is upwardly corrected by a factor determined from LASNEX[32] simulations. The LASNEX simulations determine the correction factor by calculating the temperature under the conditions of each experiment and repeating the calculation with the interaction beam off. The ratio of the temperature at the center of the interaction beam to that when the beam is absent is calculated for each case and the temperature measured in the experiment is multiplied by this factor to determine the temperature in the region of the interaction beam. This correction is largest at the lowest heater powers where it is less than 30%. The light scattered by SRS is measured in a series of shots with varying electron temperature and plotted versus the corrected temperature in Fig. 4.

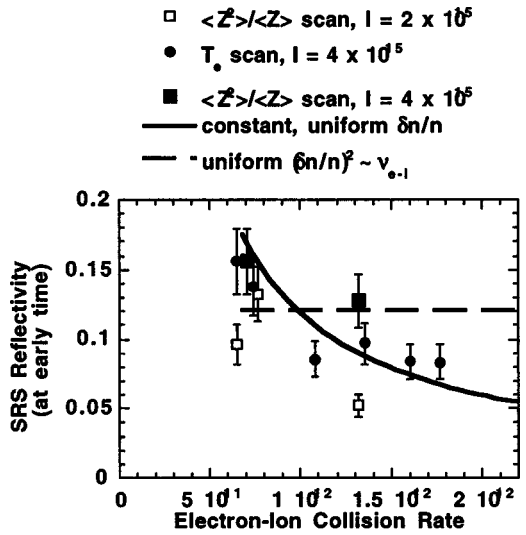

FIG. 5. Laser reflectivity from an $f/4.3$ beam due to SRS vs the electron-ion collision rate from experiments in 11% critical density targets with varying ion species concentration ($\langle Z^2\rangle/\langle Z\rangle$), and with varying electron temperature shown in Fig. 3.

The SRS measurements shown in Fig. 4 indicate that the percent reflectivity of the beam varies weakly with plasma electron temperature over the range of 1.5–3.0 keV in spite of the fact that the Landau damping rate in a Maxwellian plasma varies by more than an order of magnitude over this range. However, such a weak dependence on wave amplitudes on the linear wave damping rate may be consistent with nonlinear saturation mechanisms discussed in the following.

V. EFFECT OF ELECTRON-ION COLLISIONS ON SRS

Because the variation of the SRS with temperature is so weak it cannot be solely attributed to a temperature dependence of the collisionless damping of the scattering plasma wave. Thus, the temperature dependence due to other temperature dependent processes is considered. As mentioned earlier, the collisional absorption of the out going Raman light by inverse bremsstrahlung absorption may make the observed scattering dependent on electron ion collisions. This dependence on electron-ion collisions is tested experi-

Downloaded 21 Nov 2003 to 128.32.113.135. Redistribution subject to AIP license or copyright, see http://ojps.aip.org/pop/popcr.jsp

mentally, by varying the ion charge of the target, which will vary this rate and may also affect the plasma weakly in other ways (such as heat transport, or variation in the ion acoustic wave properties, or the trapping of electrons in the plasma wave). From the measured dependence of SRS on Z and the expected dependence of the out going light on inverse bremsstrahlung absorption, the relative importance of these other processes on SRS can be inferred. A series of further experiments were performed to determine the importance of electron-ion collisions and other Z dependent processes to the observed temperature scaling, by varying the Z of the material, while keeping the electron temperature constant. This was done by varying the average ion $Z(=\langle Z^2\rangle/\langle Z\rangle)$ by adding up to 13% Xe (by molecular number) to the C_5H_{12} gas. The heater and interaction beams were as described for the temperature dependence experiments above, with the heater beams at maximum power. Measurements of the gas bag temperatures were obtained by x-ray spectroscopic analysis of the Ar emission (with 1% Ar impurity[29]) spectra and showed that the peak (in time) of the temperature was between 3.3 and 2.9 (± 0.6) keV for gas bags with no Xe and 13% Xe (respectively), which is consistent with the predictions of LASNEX simulations. At the same time the simulations indicate that the Xe was stripped to a charge state of $Z\sim 40$ so that the electron density varied by less than 0.5% over the same range of dopant concentrations. The slightly lower temperature upon adding Xe is ascribed to greater radiative cooling $\sim Z^2$. Thus these targets provide nearly independent adjustment of $\langle Z^2\rangle/\langle Z\rangle$ and electron temperature. This allows the effect of a change in electron-ion collisions and other Z dependent processes to be separated from the effect of a temperature change, which will affect SRS both through a change in the electron ion-collision rate, and through collisionless damping, and can clarify the relative roles of the collisional absorption of the out going light and variation of the Langmuir wave Landau damping rate on the scattered SRS measurements.

Data on SRS scattering are taken from targets doped with 13% Xe and from beam intensities equivalent to those in the temperature scaling experiment ($I=4\times 10^{15}\,\mathrm{W/cm^2}$) and at a lower intensity ($I=2\times 10^{15}\,\mathrm{W/cm^2}$). It is observed that the variation of the measured SRS scattering with $\langle Z^2\rangle/\langle Z\rangle$ is also quite weak, and is not significantly different from variation of SRS with electron temperature, when both are considered to affect only the electron ion collision rate. This is seen in Fig. 5 from the fact that the data from the two different experiments do not have significantly different values when compared at the same value of electron ion collision frequency, and the same laser beam intensity (i.e., the data in Fig. 5 correlate with a particular collision rate regardless of whether the atomic number is being varied or the electron temperature is being varied to obtain that collision rate). The curves in Fig. 5 represent an estimate of effect on the SRS of the inverse bremsstrahlung absorption of the scattered light for two idealized models of a spatially uniform scattering wave, one in which the mean square amplitude of the scattering wave is independent of the collision rate (labeled ''constant, uniform $\delta n/n$''), and one in which it is linearly proportional to collision frequency (labeled ''uniform $(\delta n/n)^2\sim \nu_{e,I}$''). The estimates assume that the out going light is reabsorbed by inverse bremstrahlung in a homogeneous plasma, and that the total scattered power is the sum of the scattered power from each region which has been attenuated exponentially along the path to the plasma edge (i.e., incoherent scattering with phase dependence averaged). So when the plasma and wave amplitude are uniform and the plasma is much thicker than the inverse bremsstrahlung absorption rate κ,

$$P_{\mathrm{scat}}\propto \int_0^L P_{\mathrm{inc.}}(x)\partial n^2(x)\exp(-\kappa(L-x))dx\approx \frac{P_{\mathrm{inc.}}\partial n^2}{\kappa}, \tag{1}$$

which gives the solid line in Fig. 5. In the case where the wave amplitude ∂n^2 is portional to the electron ion collision rate the scattered power will not depend on the collision rate because it cancels with the dependence of κ in the denominator. The fact that the dependence of the data on collision rate is within the range of the first of these two estimates (when a single amplitude scale factor is adjusted to fit the data) suggests that much of the dependence of SRS on temperature observed in Fig. 4 is due to the variation of the inverse bremsstrahlung absorption rate of the out going light with the electron temperature, and that all other temperature dependent processes have a still smaller effect on the SRS temperature dependence. The intensity scaling in Xe doped targets is also observed to show the SRS reflectivity is close to linear with intensity as in the above-mentioned pure CH targets.

VI. MODELING

SRS is a three wave resonant instability in which the incident large amplitude coherent laser light wave decays into a backward propagating light wave and a Langmuir wave. The waves must maintain temporal and spatial phase coherence, which imposes the well-known frequency and wavenumber matching conditions, $\omega_0=\omega_r+\omega_p$ and $k_0=k_r+k_p$. Here, the subscripts $0,r,p$ refer to the incident light, the reflected Raman light, and the Langmuir wave, respectively. We restrict our attention to convective amplification because the threshold is lower than that for absolute instability and the convective gain in these experiments is sufficient to reflect a large fraction of the light absent nonlinear processes. The convective temporal threshold, $\gamma_{0,\mathrm{SRS}}^{2,\mathrm{th}}=\nu_r\nu_p$ is easily satisfied where γ_0 is the SRS convective growth rate and ν_r and ν_p are the damping rates of the Raman reflected light and the Langmuir wave, respectively. More important is the convective gain exponent,

$$G(\omega_r)=\frac{1}{4}\frac{k_p^2v_0^2}{v_{gr}\omega_r}\int_{\mathrm{path}} dz\,\mathrm{Im}\left(\frac{\chi_e(1+\chi_i)}{\epsilon(k_r-k_0,\omega_r-\omega_0)}\right) -2\int_{\mathrm{path}} dz\,\frac{\nu_r}{v_{gr}}, \tag{2}$$

where $\epsilon=1+\chi_e+\chi_i$ is the dielectric function for the plasma wave of frequency $\omega_r-\omega_0$ and wavenumber k_0-k_r. The gain peaks at those frequencies for which the dielectric function is nearly zero, i.e., when the light scatters from a natural

Downloaded 21 Nov 2003 to 128.32.113.135. Redistribution subject to AIP license or copyright, see http://ojps.aip.org/pop/popcr.jsp

mode of oscillation of the plasma, such as an ion acoustic or Langmuir wave. For ponderomotively driven SBS, the intensity gain exponent is

$$G_{\mathrm{SBS}}=\frac{1}{8}\frac{v_0^2}{v_e^2}\frac{n_e}{n_c}\frac{\omega_a}{\nu_a}\frac{\omega_0}{v_{gb}}L_{\mathrm{SBS}}-2\frac{\nu_{\mathrm{abs}}^b}{v_{gb}}L$$

$$=2\left(\frac{\gamma_{0,\mathrm{SBS}}^2}{\nu_a}-\nu_{\mathrm{abs}}^b\right)\frac{L_{\mathrm{SBS}}}{v_{gb}}-2\nu_{\mathrm{abs}}^b L_{nr} \quad (3)$$

and for SRS, it is

$$G_{\mathrm{SRS}}=\frac{1}{8}\frac{k_p^2 v_0^2}{\omega_0\omega_r}\frac{\omega_p}{\nu_p}\frac{\omega_0}{v_{gr}}L_{\mathrm{SRS}}-2\frac{\nu_r}{v_{gr}}L$$

$$=2\left(\frac{\gamma_{0,\mathrm{SRS}}^2}{\nu_p}-\nu_r\right)\frac{L_{\mathrm{SRS}}}{v_{gr}}-2\nu_r L_{nr}, \quad (4)$$

where the fluid limit of the plasma dispersion function has been used. Here, v_0 is the oscillatory velocity of an electron in the laser electric field, and L_{SBS} or L_{SRS} is the smaller of the plasma length or, in an inhomogeneous plasma, the length over which the three-wave resonance for SBS or SRS is maintained. Here, ω_a and ν_a are the local acoustic frequency of the least damped mode and acoustic wave damping rate, respectively. In the pF3d modeling discussed in the following, there is a 0.5 mm scale length density gradient region in which little SRS growth occurs because there $L_{\mathrm{SRS}}=\nu_e/\omega_{pe}L_n\sim 50\,\mu$m for the SRS interaction. The effective absorption length L_{nr} is much longer and, as discussed previously, the scattered SRS light can be absorbed by inverse bremstrahlung as it propagates from the resonant region to the detector. The group velocities of the laser light and the Brillouin and Raman scattered light are v_{g0}, v_{gb}, v_{gr}, respectively, and $v_{g0,r}=c^2k_{0,r}/\omega_{0,r}$, $v_{gb}=C_s$, and $v_{gl}=3k_l v_e^2/\omega_l$ in the fluid limit. The important parameters are the laser intensity, the electron temperature, the electron density, the relevant damping rate, and the length L_{SRS} or L_{SBS} over which the matching conditions are maintained. If $k_p\lambda_{\mathrm{De}}$, <0.2, the Landau damping is very small but collisional damping remains. In National Ignition Facility (NIF) relevant 3 to 6 keV plasmas, this collisional damping rate is very weak; if it were the only damping mechanism SRS would be absolutely unstable. In the second form of the SBS and SRS gain, one sees that the gain is zero in the resonant region at the convective temporal threshold.

For the parameters of the intensity scaling experiments, C_5H_{12}, it is instructive to evaluate typical rates. The convective threshold intensity is $2.6\times10^{13}\,\mathrm{W/cm^2}$, the energy spatial absorption rate is 0.26/mm for the incident light and 0.73/mm for the SRS light at the wavelength for optimum gain ($\lambda_{\mathrm{SRS}}=564\,\mathrm{nm}$) in a $0.1n_c$, 2.5 keV plasma. Thus, in 1 mm, half the SRS light and one-quarter of the incident light would be absorbed for these parameters. The convective SRS intensity gain exponent (without the absorption correction) is 56 for $L=1$ mm at a laser intensity of $2\times10^{15}\,\mathrm{W/cm^2}$. Even at $3\times10^{14}\,\mathrm{W/cm^2}$, the SRS light damping rate makes a small correction to the gain exponent. The SRS gain exponent is 35 for a $0.1n_c$, 3 keV, 1 mm long plasma and 18 for a $0.07n_c$, 2.5 keV, 1 mm long plasma. Because a gain exponent of 20 is sufficient for pump depletion for a plane wave pump laser and nonuniform RPP beams can scatter more for the same spot-averaged intensity, these experiments in nearly 2 mm long plasmas are testing the nonlinear scaling of SRS, not the behavior near threshold.

The threshold Langmuir wave charge density $\delta n_{\mathrm{th}}^{\mathrm{LDI}}$ for driving the LDI is given by

$$\left|\frac{\delta n_{\mathrm{th}}^{\mathrm{LDI}}}{n_e}\right|^2=16(k\lambda_{\mathrm{De}})^2\frac{\nu_e}{\omega_1}\frac{\nu_a}{\omega_a},$$

where n_e is the background density, $\nu_e=\nu_e^c+\nu_e^{\mathrm{L}}$ is the sum of the collisional damping rate, $\nu_e^c=1/2\nu_{ei}\omega_{pe}^2/\omega_1^2$, and the Landau damping rate ν_e^{L} of the Langmuir wave of frequency ω_1. The threshold depends on the damping rate of the acoustic wave and thus, if the damping rate of the acoustic wave were increased while other plasma parameters are kept constant, the Langmuir wave can be driven to larger amplitude and more SRS would be expected for the same linear gain exponent.

The observed *scaling* with intensity is consistent with theories which describe the saturation of the Langmuir wave by secondary decays[7–9] and predict a linear dependence of reflectivity on laser intensity, ion wave damping rate, the electron temperature, and the plasma length $R_{\mathrm{SRS}}\sim I_{\mathrm{L}}T_e\nu_a L^{\beta}/\omega_a$. The length dependence is determined by the axial coherence of the interaction with $\beta=3$ for complete coherence and $\beta=1$ for incoherence. Note the lack of dependence of the saturated reflectivity on the linear electron damping rate is consistent with the similar reflectivity for 7% and 10% critical plasma shown in Figs. 3(a) and 3(b) and the lack of temperature dependence shown in Fig. 4.

Under the conditions studied here, the high laser beam intensities, long scale lengths, and high plasma temperature SRS are expected to produce large amplitude Langmuir waves that may be affected by a variety of non-linear processes. These processes include filamentation of the incident laser beam, that will substantially modify its intensity profile, and a variety of fluid and kinetic non-linearities of the Langmuir waves, including secondary decays and particle trapping. To assess more quantitatively the importance of nonlinear effects, the experimental conditions are simulated using PF3D[2324]. The plasma is simulated in two dimensions with a uniform density region of 1 mm where $n_e=0.1n_c$ and most of the SRS gain occurs. In addition, the plasma expansion region outside the density plateau is simulated with a density that starts from 0.035 nc and rises to 0.16 nc over a length of 0.52 mm. Thus, the effects of the plasma induced incoherence[33] and the reabsorption of the SRS light are included. The flow velocity in the plateau is initially zero; in the expansion region it flows outward toward the laser with a linear gradient. The flow at the peak density of the blast wave is inward and sonic, $T_e=2.5\,\mathrm{keV}$ and $T_i=600\,\mathrm{eV}$ in the plateau region. The laser beam, the Raman scattered light, and the Langmuir wave are all propagated through the plasma with the time and spatial variation of all waves accounted for. The incident laser field has an intensity distribution appropriate for the random phase plates and lens *f*-number used in the experiment. The SRS scattered light

Downloaded 21 Nov 2003 to 128.32.113.135. Redistribution subject to AIP license or copyright, see http://ojps.aip.org/pop/popcr.jsp

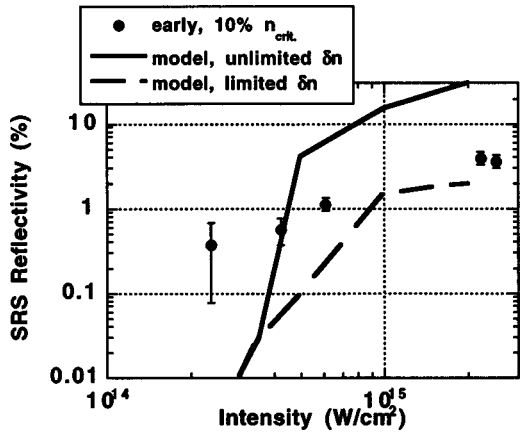

FIG. 6. Two-dimensional fluid simulations (PF3D) are used to determine the laser beam intensity profile in the presence of filamentation for the conditions of the $f/8$ beam and 0.1 critical density plasma experiments shown in Fig. 2(a). SRS reflectivity calculated from these laser and plasma profiles is plotted vs laser intensity and shown to scale rapidly up with intensity at values comparable to those where the onset of SRS is observed. Calculations where the wave amplitude is limited are also shown as discussed in text.

grows both from thermal Langmuir fluctuations and bremsstrahlung. The frequency shifts of the normal mode frequencies due to localized heating or density variations produced by ponderomotive forces of all the waves are accounted for. Shown in Fig. 6, the simulated SRS reproduces the onset of SRS at an intensity of a few $\times 10^{14}\,\mathrm{W/cm^2}$, and grows up to 10% or greater at high intensity when the damping rates are the linear ones calculated for the plasma parameters appropriate at 1 ns. It is also observed that the simulated reflectivity is two or three times higher than the late-time measured ones and more than five times higher than the early time measured ones in the high intensity cases. Let us assume that non-linear processes are operating to limit the Langmuir wave amplitude and the scattering. Decay of the Langmuir wave through LDI[7–9] is one possible mechanism, and we have investigated its possible importance by introducing into the simulations an empirical amplitude dependent damping factor that makes the Langmuir wave damping increase sharply when its amplitude exceeds the threshold for LDI. Inclusion of the LDI enhanced damping rate does not reduce the scattered light unless the threshold for non-linear damping is reduced to $\sim$3% of the LDI threshold. The reason is that, in the region of maximum SRS gain, the amplitude of the Langmuir wave has a rms value ten times smaller than the LDI threshold value, $\delta n_{\mathrm{th}}^{\mathrm{LDI}}/n_e \sim 0.1$. Figure 6 shows that lowering the threshold 300 times reduces the simulated SRS below the measured SRS. Hence, the remaining discrepancies between the simulation and the measurements cannot be explained by LDI unless the threshold is much lower than it would be in a Maxwellian plasma. The observations of weak intensity dependence may also be consistent with saturation of the Langmuir wave by particle trapping and subsequent detuning of the wave.[20] The latter theories have the advantage that they also describe the reduction of the Langmuir wave damping rate[34] at the onset of SRS which may be consistent with our observations of significant SRS at intensities as low as $3\times 10^{14}\,\mathrm{W/cm^2}$. However it may be more difficult to explain previous observations that SRS depends on ion acoustic wave damping with particle trapping theories that do not inherently involve ion-wave dynamics. Some simulations show[23] and some data suggest that SBS can reduce the amount of SRS. At low intensity the SBS reflectivity in these experiments is larger than the SRS and comparable to the SRS at the higher intensities for both early and late times. The SRS reflectivity increases with intensity for both early and late times with about the same onset intensity and similar values. On the other hand, the early time SBS is independent of intensity which also suggests a nonlinear saturation. The late-time SBS increases with intensity with an onset intensity similar to the SRS one and reflectivities similar to the SRS ones. This behavior does not appear to support a model where SBS suppresses SRS. Moreover, the SBS data themselves need a nonlinear saturation model. Thus, although an influence of SBS on SRS or vice versa cannot be ruled out, we have no viable model to offer in this case.

The variation with the electron-ion collision frequency can be understood in terms of the reabsorption of the SRS light in the plasma expansion region where SRS is inhibited by the density gradient detuning discussed earlier. For example, in the expansion region used in the pF3d simulations 35% of the SRS light is absorbed for no Xe whereas 70% is absorbed for 13% Xe because, as shown in Fig. 5, the absorption rate increases threefold.

VII. CONCLUSIONS

These experiments have shown that the scaling of SRS reflectivity with incident beam intensity in large scale, hot plasmas shows only an approximately linear dependence with $f/8$ beams, and the scaling with electron temperature is also weak in experiments with $f/4.3$ beams, with a temperature dependence of the reflectivity that could be entirely described by the temperature dependence of the inverse bremstrahlung absorption of the backreflected light. The intensity scaling results occur in the presence of SBS reflectivity that is less than 3% and weakly varying. These results may be consistent with Langmuir waves that are saturated by nonlinear mechanisms. Further experiments in Xe doped plasmas allowed the electron-ion collision rate to be varied while the electron temperature was held constant, and showed that variation of the electron-ion collision rate can account for most of the observed dependence of SRS on electron temperature suggesting little temperature dependence of SRS by collisionless processes such as Landau damping.

[1] J. D. Lindl, Phys. Plasmas **2**, 3933 (1995).
[2] L. V. Powers, R. L. Berger, R. L. Kauffman, B. J. MacGowan *et al.*, Phys. Plasmas **2**, 2473 (1995).
[3] B. J. MacGowan, B. B. Afeyan, C. A. Back, R. L. Berger *et al.*, Phys. Plasmas **3**, 2029 (1996).
[4] R. K. Kirkwood, B. B. Afeyan, W. L. Kruer, B. J. MacGowan, J. D. Moody, D. S. Montgomery, D. M. Pennington, T. L. Weiland, S. C. Wilks *et al.*, Phys. Rev. Lett. **77**, 2706 (1996).
[5] J. C. Fernández, J. A. Cobble, B. H. Failor, D. F. DuBois, D. S. Montgomery, H. A. Rose, H. X. Vu, B. H. Wilde, M. D. Wilke, and R. E. Chrien, Phys. Rev. Lett. **77**, 2702 (1996).
[6] E. A. Williams, R. L. Berger, R. P. Drake, A. M. Rubenchik, B. S. Bauer,

Downloaded 21 Nov 2003 to 128.32.113.135. Redistribution subject to AIP license or copyright, see http://ojps.aip.org/pop/popcr.jsp

D. D. Meyerhofer, A. C. Gaeris, and T. W. Johnston, Phys. Plasmas **2**, 129 (1995).
[7]S. J. Karttunen, Plasma Phys. **22**, 151 (1980).
[8]T. Kolber, W. Rozmus, and V. T. Tikhonchuk, Phys. Fluids B **5**, 138 (1993).
[9]B. Bezzerides, D. F. Dubois, and H. A. Rose, Phys. Rev. Lett. **70**, 2569 (1993).
[10]S. Depierreux, J. Fuchs, C. Labaune, A. Michard, H. A. Baldis, D. Pesme, S. Hüller, and G. Laval, Phys. Rev. Lett. **84**, 2869 (2000).
[11]C. Labaune, H. A. Baldis, B. S. Bauer, V. T. Tikhonchuk, and G. Laval, Phys. Plasmas **5**, 234 (1998).
[12]C. G. R. Geddes, R. K. Kirkwood, S. H. Glenzer, B. I. Cohen, and P. E. Young, ''Observation on ion wave decay products of Langmuir waves generated by stimulated Raman scattering in ignition scale plasmas,'' Phys. Plasmas (to be published).
[13]D. S. Montgomery, J. A. Cobble, J. C. Fernández, R. J. Focia, R. P. Johnson, N. Renard-LeGalloudec, H. A. Rose, and D. A. Russell, Phys. Plasmas **9**, 2311 (2002).
[14]R. K. Kirkwood, D. S. Montgomery, B. B. Afeyan, J. D. Moody *et al.*, Phys. Rev. Lett. **83**, 2965 (1999).
[15]A. B. Langdon, Phys. Rev. Lett. **44**, 575 (1980).
[16]B. B. Afeyan, A. E. Chou, J. P. Matte, R. P. J. Town, and W. J. Kruer, Phys. Rev. Lett. **80**, 2322 (1998).
[17]S. H. Glenzer, W. Rozmus, B. J. MacGowan, K. G. Estabrook *et al.*, Phys. Rev. Lett. **82**, 97 (1999).
[18]S. Brunner and E. J. Valeo, Phys. Plasmas **9**, 923 (2002).
[19]T. M. O'Neil, Phys. Fluids **8**, 2255 (1965).
[20]G. J. Morales and T. M. O'Neil, Phys. Rev. Lett. **28**, 417 (1972).
[21]H. X. Vu, D. F. DuBois, and B. Bezzerides, Phys. Rev. Lett. **86**, 4306 (2001).
[22]E. J. Valeo and S. Brunner, ''Trapped-particle instability leading to bursting in stimulated raman scattering simulations,'' in preparation.
[23]R. L. Berger, C. H. Still, E. A. Williams, and A. B. Langdon, Phys. Plasmas **5**, 4337 (1998).
[24]R. L. Berger, E. Lefebvre, A. B. Langdon, J. E. Rothenberg, C. H. Still, and E. A. Williams, Phys. Plasmas **6**, 1043 (1999).
[25]D. S. Montgomery, B. B. Afeyan, J. A. Cobble, J. C. Fernández, M. D. Wilke, S. H. Glenzer, R. K. Kirkwood, B. J. MacGowan, J. D. Moody, E. L. Lindman, D. H. Munro, B. H. Wilde, H. A. Rose, D. F. Dubois, B. Bezzerides *et al.*, Phys. Plasmas **5**, 1973 (1998).
[26]J. C. Fernández, J. A. Cobble, D. S. Montgomery, M. D. Wilke, and B. B. Afeyan, Phys. Plasmas **7**, 3743 (2000).
[27]H. A. Rose and D. F. DuBois, Phys. Rev. Lett. **72**, 2883 (1994).
[28]R. L. Berger, B. F. Lasinski, A. B. Langdon, T. B. Kaiser, B. B. Afeyan, B. I. Cohen, C. H. Still, and E. A. Williams, Phys. Rev. Lett. **75**, 1078 (1995); erratum, *ibid.* **76**, 3239 (1996).
[29]S. H. Glenzer, L. M. Divol, R. L. Berger, C. Geddes, R. K. Kirkwood, J. D. Moody, E. A. Williams, and P. E. Young, Phys. Rev. Lett. **86**, 2565 (2001).
[30]D. H. Kalantar, D. E. Klem, B. J. MacGowan, J. D. Moody, D. S. Montgomery, D. H. Munro, T. D. Shepard, G. F. Stone, B. H. Failor, and W. W. Hsing, Phys. Plasmas **2**, 3161 (1995).
[31]S. H. Glenzer, T. L. Weiland, J. Bower, A. J. MacKinnon, and B. J. MacGowan, Rev. Sci. Instrum. **70**, 1089 (1999).
[32]G. Zimmerman and W. Kruer, Plasma Phys. Controlled Fusion **2**, 85 (1975).
[33]J. Fuchs, C. Labaune, S. Depierreux, H. A. Baldis, A. Michard, and G. James, Phys. Rev. Lett. **86**, 432 (2001); A. Schmidt and B. B. Afeyan, Phys. Plasmas **5**, 503 (1998).
[34]D. D. Mourenas, Phys. Plasmas **6**, 1258 (1999).

Downloaded 21 Nov 2003 to 128.32.113.135. Redistribution subject to AIP license or copyright, see http://ojps.aip.org/pop/popcr.jsp